

## METHODS

### Fish sampling

Threespine sticklebacks of the Japanese sympatric pair were collected with seine nets and minnow traps in Lake Akkeshi, the Bekanbeushi River, and Hyoton Pond in May–July of 2003–2008, as described previously<sup>19,36</sup>. Fish collected in 2007 and 2008 were used for cytogenetic analysis, fish collected in 2006 and 2007 were used for population genetic analysis, fish collected in 2005, 2007 and 2008 were used for mate choice experiments, and fish collected in 2003 were used for making crosses. Allopatric Japan Sea fish were collected in 2008 from the Cape of Bankei on the western coast of Hokkaido and used only for cytogenetic analysis.

### Japan Sea linkage map construction

A Japan Sea female was crossed to a Japan Sea male to make a pure Japan Sea cross. The parents were genotyped with six species-diagnostic markers<sup>19</sup> to confirm that they were of the Japan Sea form. Progeny were grown for one year, and then sex was determined by visual inspection of the gonads. To create a linkage map of the sex chromosomes, 46 fish (19 males and 27 females) were genotyped with nine microsatellite markers on LG9 (*Stn102*, *Stn105*, *Stn107*, *Stn108*, *Stn113*, *Stn114*, *Stn115*, *Stn116*, *Stn225*) and 10 microsatellite markers on LG19 (*Stn186*, *Stn187*, *Stn188*, *Stn192*, *Stn256*, *Stn274*, *Stn284*, *Stn303*, *Cyp19b*, *19.07Mbp*). The primer sequences of all *Stn* markers are available through GenBank; primer pair 5'-AGCGAACAGCTTCAACTTC-3' and 5'-CGACATCCCAAACAGTTTCC-3' amplifies a microsatellite near the *Cyp19b* gene and primer pair 5'-GCGTCCGTTCTCTACATGG-3' and 5'-AGGAGGGTTCATCTTCATGC-3' amplifies a microsatellite at 19.07 Mbp on the X chromosome assembly<sup>22</sup>. Genetic maps of LG9 and LG19 were created using JoinMap 3.0 software<sup>33</sup>.

### Cytogenetics

Karyotyping and fluorescence *in situ* hybridization (FISH) were conducted as previously described<sup>22</sup>. The LG9 probe is a bacterial artificial chromosome (BAC) from the CHORI-213 library (69J04) that contains the *Stn114* microsatellite marker on LG9. The LG19 probe is a CHORI-213 BAC (188J19) that is near the *Stn186* microsatellite marker on LG19<sup>22</sup>. The LG9 BAC was labeled with Alexa fluor 568 nm (magenta in FISH images), and the LG19 BAC was labeled with Alexa fluor 488 nm (green in FISH images). Two Pacific Ocean males (10 metaphases), two Pacific Ocean females (8 metaphases), two sympatric Japan Sea males (11 metaphases), one sympatric Japan Sea female (9 metaphases), two allopatric Japan Sea males (17 metaphases), and three allopatric Japan Sea females (24 metaphases) were analyzed.

### Population genetic analysis

In total, 601 fish (317 adults, 284 juveniles) were collected in June–July 2006, and 368 fish (105 adults, 263 juveniles) were collected in June–July 2007 from four sites in Akkeshi (Lake Akkeshi, Mid1, Mid2, Upstream; Fig. 2). These fish were genotyped with twelve microsatellite markers (Supplementary Table 4) on eight linkage groups, including four species-discriminatory markers<sup>19</sup>. These markers have allele sizes consistent with the stepwise mutation model and are in Hardy-Weinberg equilibrium within forms (GenePop<sup>37</sup> exact test;  $P > 0.05$  after Bonferroni correction).

Genotyping data were analyzed with STRUCTURE<sup>38</sup>. Since some of the markers are on the same linkage group (Supplementary Table 4), linkage information (physical location of markers in the public stickleback genome assembly) was included in the input file for STRUCTURE analysis. We estimated the number of clusters in the data by running three simulations for each  $K$  value from  $K = 1$  through  $K = 8$  to calculate the mean log probability of data ( $L(K)$ ) and by using the *ad hoc* statistic  $\Delta K$ , which is based on the rate of change in  $L(K)$  between successive  $K$  values<sup>39</sup> (Supplementary Fig. 2a). Parameters were estimated after 200,000 iterations, following a burn-in of 25,000 iterations. STRUCTURE was then used to determine the probability that an individual belongs to the Japan Sea or Pacific Ocean form. To confirm the presence of two genetic clusters, the pairwise genetic distance (Dps) between individual adult fish collected in 2006 ( $n = 317$ ) was calculated from the proportion of shared alleles using MSA software<sup>40</sup>. Then, R statistical software<sup>41</sup> was used to conduct principal coordinate (PCo) analysis on the genetic distance matrix (Supplementary Fig. 2b).

### Components of reproductive isolation

We first quantified the relative contributions of five potential isolating barriers (geographical isolation, temporal isolation, behavioural isolation, intrinsic hybrid inviability (hatching rate), and hybrid sterility). We first used the method of Ramsey *et al.*<sup>42</sup>, which is an extension of that of Coyne & Orr<sup>43</sup> and has been widely used in many systems<sup>42,44-46</sup>. For prezygotic isolating barriers, the strength of each barrier ( $RI$ ) was calculated as  $RI_{prezygotic} = 1 - (\text{number of heterospecific matings}/\text{number of homospecific matings})$ . For postzygotic isolating barriers,  $RI$  was calculated as  $RI_{postzygotic} = 1 - (\text{hybrid fitness}/\text{parental fitness})$ . This index reflects the strength of each isolating barrier: a value of 1 indicates complete isolation; a value of 0 indicates the absence of reproductive isolation; negative values indicate that hybridization is favoured. Next, under the assumption that each isolating barrier acts sequentially and independently, the relative contribution of each barrier was calculated using an Excel spreadsheet developed by Ramsey *et al.*<sup>42</sup>. Data on geographical isolation is described below. Data on other isolating barriers were taken from published literature<sup>19,36,47-49</sup>. We conducted the analysis both including and excluding geographical isolation, which allowed us to calculate the relative importance of isolating barriers in the hybrid zone.

We also calculated the expected frequency of reciprocal F1 hybrids after the action of each sequentially acting isolating barrier following Martin & Willis<sup>50</sup>. If a particular isolating barrier is very strong, the expected frequency of hybrids should decrease after the action of that barrier. In contrast, if hybridization is favoured at a particular stage, the expected frequency of hybrids will increase after the action of that barrier. The frequency of reciprocal hybrid was calculated as the fraction of hybrids (Japan Sea female x Pacific Ocean male) among progeny of Japan Sea females ( $q_{JP}$ ) and the fraction of hybrids (Pacific Ocean female x Japan Sea male) among progeny of Pacific Ocean females ( $q_{PJ}$ ). In the next sections, we provide the details for calculating the expected frequencies of hybrids, following Martin & Willis<sup>50</sup>.

### Geographical isolation

Previous extensive field surveys of the Bekaubeushi River drainage identified four main breeding sites (Lake, Mid1, Mid2, and Upstream; Fig. 2)<sup>47</sup>. We have not yet found any other breeding sites within the lake, but we cannot exclude the possibility that there are some other minor breeding sites in some small tributaries of Bekaubeushi River. At each breeding site, fish were collected by the same sampling method: setting eight minnow traps (25 cm x 25 cm x 45

cm with 4 mm mesh) for 30 min as well as hauling a seine net (10 m-wide with 2 mm mesh) at one compartment ( $\sim 300 \text{ m}^2$ ) of each breeding ground for three times on June 27, 2006 and again on July 13, 2006. Adult fish collected on these two days ( $n = 317$ ) were combined and analyzed together using STRUCTURE (see above). The number of fish collected during these two periods were summed and used as a proxy for the population size at each site. Because this data based on single-area sampling may not reflect the real population size, our estimates of geographical isolation should be interpreted with caution. Fish with  $> 0.1$  hybridity were excluded from the subsequent analysis (only 2/ 317 fish). Sex was determined by visual inspection of the gonads or detection of the male specific *Idh* polymorphism<sup>21</sup>. In the absence of any isolating barriers, the expected frequency of females mating with heterospecific males should simply equal the frequency of heterospecific males. Thus, the expected frequency of Pacific Ocean females mating with Japan Sea males is 0.59 (= frequency of Japan Sea males among all males) and that of Japan Sea females mating with Pacific Ocean males is 0.41 (= frequency of Pacific Ocean males among all males). Because geographical isolation should reduce heterospecific encounters, we next calculated the frequency of heterospecific encounters in the presence of geographical isolation for Japan Sea females ( $q_{1,JP}$ ) and Pacific Ocean females ( $q_{1,PJ}$ ). Here, the encounter rate was first calculated for individual breeding sites and summed after weighing the relative population size of females in each site, as determined above.

#### Temporal isolation

The timing of breeding for each form was studied by Kume<sup>47</sup>, where fish were collected with minnow traps at three different time points in 2003 (May 11-20, June 11-20, and June 21-30) from two breeding sites (Lake and Mid1; Fig. 2). The frequency of males with nuptial colour (red throat, blue eye, or blue back) was recorded for Pacific Ocean and Japan Sea males,  $m_{iP}$  and  $m_{iJ}$ , respectively on the  $i$ th observation ( $i = 1\sim 3$ )<sup>47</sup>. The fraction of gravid females observed on the  $i$ th observation among all of three observations was also recorded for Pacific Ocean and Japan Sea females,  $f_{iP}$  and  $f_{iJ}$ , respectively<sup>47</sup>. All fish were classified by visual inspection (body size and lateral plate pattern); subsequent genetic analysis of some of these fish revealed that 60/60 fish were classified correctly<sup>19</sup>. The expected frequency of reciprocal hybrids after taking temporal isolation into consideration can be calculated as:

$$q_{2,JP} = \frac{\sum_i q_{1,JP} \times f_{i,J} \times m_{i,P}}{\sum_i q_{1,JP} \times f_{i,J} \times m_{i,P} + \sum_i (1 - q_{1,JP}) \times f_{i,J} \times m_{i,J}}$$

and

$$q_{2,PJ} = \frac{\sum_i q_{1,PJ} \times f_{i,P} \times m_{i,J}}{\sum_i q_{1,PJ} \times f_{i,P} \times m_{i,J} + \sum_i (1 - q_{1,PJ}) \times f_{i,P} \times m_{i,P}}$$

#### Behavioural isolation

In the presence of behavioural isolation, a non-random proportion of encounters between breeding females and breeding males results in mating. To estimate the strength of behavioural isolation, we used data from our previous laboratory female mate choice trials<sup>19</sup>. Given

$$a = \frac{\text{heterospecific mating rate (JS female x PO male)}}{\text{homospecific mating rate (JS female x JS male)}} \text{ and}$$

$$b = \frac{\text{heterospecific mating rate (PO female x JS male)}}{\text{homospecific mating rate (PO female x PO male)}} ,$$

the expected frequencies of reciprocal F1 hybrids can be calculated as:

$$q_{3,JP} = \frac{q_{2,JP} \times a}{q_{2,JP} \times a + (1 - q_{2,JP})} \text{ and } q_{3,PJ} = \frac{q_{2,PJ} \times b}{q_{2,PJ} \times b + (1 - q_{2,PJ})} .$$

### Hatching rate

Published data on the hatching rates of *in vitro* fertilized eggs of hybrid crosses and parental crosses were used<sup>48,49</sup>. These data are based on fish collected from nearby sympatric regions (Tokachi or Kushiro Rivers). Given

$$c = \frac{\text{hybrid viability (JS female x PO male)}}{\text{parental viability (JS female x JS male)}} \text{ and}$$

$$d = \frac{\text{hybrid viability (PO female x JS male)}}{\text{parental viability (PO female x PO male)}} ,$$

the expected frequencies of reciprocal F1 hybrids can be calculated as

$$q_{4,JP} = \frac{q_{3,JP} \times c}{q_{3,JP} \times c + (1 - q_{3,JP})} \text{ and } q_{4,PJ} = \frac{q_{3,PJ} \times d}{q_{3,PJ} \times d + (1 - q_{3,PJ})} .$$

### Behavioural isolation in laboratory mate choice trials

For the current study, we analyzed the mating preferences of 29 Japan Sea females and 30 Pacific Ocean females in laboratory mate choice trials, which were conducted as previously described<sup>19</sup>. Data from 10 Japan Sea females and eight Pacific Ocean females tested previously were included with new data from 19 Japan Sea females and 22 Pacific Ocean females. To investigate the role of body size divergence in behavioural isolation, some of the new female mate choice trials (16/19 Japan Sea females and 14/22 Pacific Ocean females) were conducted with small Pacific Ocean males. Small males were obtained by rearing Pacific Ocean crosses in the laboratory<sup>51</sup> (10/16 of Japan Sea female choice tests and 6/14 of Pacific Ocean female choice tests) or by collecting resident freshwater forms from Hyotan Pond, Akkeshi, Japan (6/16 of Japan Sea female choice tests and 8/14 of Pacific Ocean female choice tests). Hyotan pond fish and Pacific Ocean fish are indistinguishable in body shape and mating behaviour; they only differ in body size<sup>19</sup>. Previous behavioural experiments found no significant difference in the intensity or frequency of dorsal pricking behaviour between Pacific Ocean and Hyotan Pond males<sup>19</sup>, and there were no significant differences in dorsal spine length between the forms ( $n = 38$  Pacific Ocean males and  $n = 11$  Hyotan Pond males; ANCOVA,  $F = 0.78$ ,  $P = 0.3833$  for the first dorsal spine length;  $F = 2.40$ ,  $P = 0.1303$  for the second dorsal spine length). Rearing of Pacific Ocean males in the lab had no effect on the frequency or intensity of dorsal pricking

behaviour (Mann-Whitney  $U$ -test,  $P > 0.05$ ;  $n = 10$  lab-raised small fish and  $n = 6$  wild-caught large fish). Each pair of males was tested once with a Pacific Ocean female and once with a Japan Sea female.

The relationship between the difference in male body size and female mate choice was analyzed by logistic regression. Non-parametric cubic spline analysis<sup>52</sup> gave rise to the qualitatively same result. Akaike information criterion (AIC)<sup>53</sup> was used to find that female mate choice was best explained by differences in male body size rather than any combination of absolute male and absolute female size: AIC for Pacific Ocean female choice and the Japan Sea female choice was 17.96 and 35.70, respectively. Because size-assortative mating has been reported in other sympatric species pairs<sup>51</sup>, we examined whether females chose the male with a body size that was more similar to her own. The Pacific Ocean females chose males of similar size in 15/30 trials (binomial test  $P = 1$ ), and Japan Sea females chose males of similar size in 15/29 trials (binomial test  $P = 1$ ). Thus, size-assortative mating was not observed in this study.

After the behavioural experiments, the intensity of dorsal pricking was measured by calculating the distance the male swam upward during dorsal pricking. We also recorded whether the female continued to follow the male or escaped from the male after dorsal pricking. Differences in dorsal pricking intensity and female response were tested by pair-wise comparison with the Mann-Whitney  $U$ -test, followed by Bonferroni correction; we used a non-parametric test because female response, but not dorsal pricking, showed heterogeneity of variances.

### **Behavioural isolation in the hybrid zone**

The presence of behavioural isolation was investigated in the field by comparing the expected and observed frequency of hybrids in the hybrid zone (Mid2) in 2006 and 2007. We first calculated the proportion of ancestry in the Pacific Ocean form ( $p$ ) for each fish using STRUCTURE ( $K = 2$ ). Then, we randomly picked 70 adult males and 70 adult females collected from the hybrid zone in 2006 (70 = the number of juveniles collected from the hybrid zone in 2006) and made 70 virtual mating pairs. By taking the average  $p$  for each pair, the expected  $p$  of their progeny was estimated. Next, the hybridity ( $0.5 - |0.5 - p|$ ) of the virtual progeny was calculated and compared with that of observed hybridity of juveniles actually collected from the hybrid zone. The 95 % confidence intervals for expected hybridity were determined with 1000 simulations using R statistical software<sup>41</sup>. The same analysis was conducted for the 2007 data by randomly picking 101 adult pairs collected from the hybrid zone (101 = the number of juveniles collected from the hybrid zone in 2007).

### **Genetic crosses for linkage mapping**

For the backcross, one Japan Sea female and one Pacific Ocean male were crossed to obtain an F1 hybrid family ( $J_1 \times P_1$ ). Then, female progeny of this family were crossed with males resulting from a cross between a Pacific Ocean female and another Pacific Ocean male ( $P_2 \times P_3$ ) to generate backcross progeny. An F2 intercross was made from independent grandparents: one Pacific Ocean female and one Japan Sea male were first crossed to obtain an F1 hybrid family ( $P_4 \times J_2$ ). Then, the F1 females ( $P_4 \times J_2$  females) and the F1 males ( $P_4 \times J_2$  males) were crossed to obtain F2 progeny. Both the backcross and the F2 progeny were maintained at a density of approximately one fish per 6.5 liter at 15°C. Fish were grown for ~1 year with a light cycle of 16-hr light/8-hr dark, then for 2 months with a light cycle of 8-hr light/16-hr dark, and then for a 16-hr light/8-hr dark light cycle for 1-3 months until they came into reproductive condition.



### Phenotypic analysis of genetic crosses

Analysis of courtship behaviour was conducted as described previously<sup>19</sup>. Briefly, once the male started to show signs of sexual maturation, such as red nuptial colouration, the male was put into a solitary tank. Once the male made a nest, a gravid female was put into the same tank and mating behaviour was recorded on digital videotapes for 15 minutes or until the female entered the nest. The female was taken away from the tank before she spawned to prevent the male from fertilizing the eggs. Each male was tested with at least two different females. Although Pacific Ocean, Japan Sea and hybrid females were used, each male was not necessarily tested with two different types of females, just two different individuals. However, this does not bias our conclusions (see below).

The intensity of dorsal pricking was measured by calculating the distance the male swam back during dorsal pricking with ImageJ software (<http://rsb.info.nih.gov/ij/download.html>). For 51 backcross males and 31 F2 males, dorsal pricking behaviour was observed in both the first and second experiment. The mean dorsal pricking intensity was significantly correlated between the first and the second experiments (Spearman correlation  $r = 0.725$ ,  $P < 0.001$ ,  $n = 51$  backcross males;  $r = 0.722$ ,  $P < 0.001$ ,  $n = 31$  F2 males). Furthermore, dorsal pricking intensity is independent of female type (Fig. 3b). Therefore, we took the average of the means of the first and second tests for these males (“mean dorsal pricking”). In two backcross males and 25 F2 males, dorsal pricking was observed only in one of the two tests, so we used the mean dorsal pricking value within the observed test for the “mean dorsal pricking” trait. There were 23 backcross males and 14 F2 males that did not perform any dorsal pricking in either test and were treated as missing data for the linkage analysis. For each male that performed dorsal pricking ( $n = 53$  backcross males and  $n = 56$  F2 males), the maximum distance the male swam back throughout all of the tests was used (“max dorsal pricking”).

After the behavioural experiments, each male was weighed (“body weight”) and photographed. From the photograph, the length from the snout tip until the posterior end of the caudal keel (standard length)<sup>54</sup> was measured with ImageJ software (“body length”). The length of the first dorsal spine length was measured from ethanol-fixed fish.

After euthanasia, the testes were dissected. The gonad-somatic index (GSI), a frequently used index of sexual maturation in fish<sup>54</sup>, was calculated by dividing the gonad weight by the body weight, which was then multiplied by 100 (“testis size”). Then, one testis was stored in formalin, and the other testis and one pectoral fin were used for flow cytometry. For flow cytometry, the testis was first dissociated into single cells by lysis solution of CyStain DNA 2-step kit (Partec GmbH, Münster, Germany). After filtration, cells were mixed with DAPI, a DNA-binding fluorescence dye, supplied in the kit. The fluorescence intensity of the cells was analyzed with LSR1 flow cytometer (BD Biosciences, San Jose, CA, USA) (Supplementary Fig. 7). The same procedure was also used on the right pectoral fin to calibrate for diploid cells present in the testes (Supplementary Fig. 7). The number of diploid cells and haploid cells (i.e., mature sperm) was determined with FlowJo software (Ashland, OR, USA). By dividing the number of haploid cells by the sum of the haploid and diploid cells, we calculated an index that reflects the relative amount of mature sperm (haploid cells) in the testis (“sperm number”).

### Genotyping and linkage analysis

We genotyped 76 backcross and 70 F2 intercross males, along with cross grandparents and parents, with single nucleotide polymorphism (SNP) markers using Golden Gate SNP arrays (Illumina, San Diego, CA, USA). The SNPs used for linkage mapping are derived from all

stickleback linkage groups (Supplementary Table 5). Genotypes were analyzed with BeadStudio software (Illumina, San Diego, CA, USA). None of the markers showed significant segregation distortion, except for markers on LG9 (neo-sex chromosome) and LG19 (ancestral sex chromosome) in F2 males ( $\alpha = 0.05$ ;  $\chi^2$ -test with Bonferroni correction).

We first tested for associations between genotypes at each of these SNPs and male phenotypes using the Kruskal-Wallis test implemented in MapQTL 4.0 software<sup>34</sup>. Most of the associations in the backcross were significant even after Bonferroni correction, except for body weight and max dorsal pricking (Supplementary Table 1). In the F2 intercross, none of the associations were significant after Bonferroni correction, but most were significant at the level of  $P < 0.05$  (Supplementary Table 2).

For QTL mapping in the backcross, we used 90 SNPs that were fixed within forms, but divergent between forms (i.e.  $P_1$ ,  $P_2$ ,  $P_3$  were all homozygous for one allele, while  $J_1$  was homozygous for the alternative allele), as well as 14 additional microsatellite markers (*Stn187*, *Stn274*, *Stn235*, *Stn256*, *Stn192*, *Cyp19b*, *19.07Mbp*, *Stn118*, *Stn99*, *Stn108*, *Stn385*, *Stn110*, *Stn113*, *Stn116*) and an *Idh* 3'UTR polymorphism (Kitano, unpublished data). A linkage map was constructed in JoinMap 3.0<sup>33</sup>, using a LOD threshold of 3.0 to create linkage groups that covered 19 of the 21 known stickleback chromosomes. Although linkage maps could not be made for LG3 and LG6, genotype-phenotype associations were tested for markers on these linkage groups by the Kruskal-Wallis analysis as described above. For QTL mapping of all traits except first dorsal spine length, the linkage data and male phenotypic data were then used for interval mapping in MapQTL 4.0<sup>34</sup>. For each trait, genome-wide significance thresholds ( $\alpha < 0.05$ ) were calculated by 1000 permutation tests in MapQTL 4.0<sup>34</sup>. Because spine length is correlated with body size, spine length was first ln-transformed and then mapped in R/qtl<sup>35</sup> with ln-standard length as an interacting covariate. Genome-wide significance thresholds ( $\alpha < 0.05$ ) were calculated by 1000 permutation tests in R/qtl<sup>35</sup>. A genome-wide scan for epistatic QTL was also conducted in R/qtl<sup>35</sup>. First, a LOD score comparing the full model with an interaction between QTL to the additive QTL model was calculated. Then, the genome-wide significance thresholds ( $\alpha < 0.05$ ) were calculated by 1000 permutation tests in R/qtl<sup>35</sup>.

For QTL mapping in the F2 intercross, we used 138 SNPs that were fixed within forms, but divergent between forms (i.e.  $P_4$  was homozygous for one allele, while  $J_2$  was homozygous for the alternative allele) as well as 9 additional microsatellite markers (*Stn99*, *Stn113*, *Stn186*, *Stn193*, *Stn229*, *Stn235*, *Stn295*, *Cyp19b*, and *19.07Mbp*). The resulting linkage map covered 20 of 21 stickleback chromosomes; a linkage map could not be made for LG6. To test the significance of QTL on the non-recombining regions of X chromosome in F2 males, we needed to calculate an X-chromosome-specific LOD threshold<sup>55</sup>. Therefore, we used R/qtl<sup>35</sup> for QTL mapping in the F2 males, which can incorporate sex chromosome information and calculate sex chromosome-specific LOD thresholds<sup>55</sup>. Because there are two X chromosomes (LG9 and LG19) segregating in the F2 intercross, we conducted QTL mapping twice, once with LG9 being treated as the X and once with LG19 being treated as the X. In the backcross, we did not have to calculate an X-chromosome-specific LOD threshold, but we confirmed that using R/qtl gave rise to the same results as using MapQTL 4.0 (Supplementary Fig. 4).

### Sex ratio meiotic drive test

If the male sterility locus is linked to a meiotic drive factor, the transmission ratio of the Japan Sea-X and Pacific Ocean-Y from an F1 hybrid male (JP = Japan Sea female x Pacific male) should be biased, leading to a bias in the ratio of female to male progeny. Although the hatching

rate of eggs fertilized by JP hybrid males is greatly reduced<sup>49</sup>, some progeny are produced (Supplementary Table 3). Thus, we used sperm from four different JP hybrid males to fertilize eggs from three different lab-reared Pacific Ocean females (PP) and a wild-caught Japan Sea female (JS). The sex ratios of the hatched fry were determined by PCR analysis of a polymorphism in the *Idh* 3'UTR<sup>21</sup>. Sex-ratio bias was tested by a two-tailed binomial test.

## SUPPLEMENTARY DISCUSSION

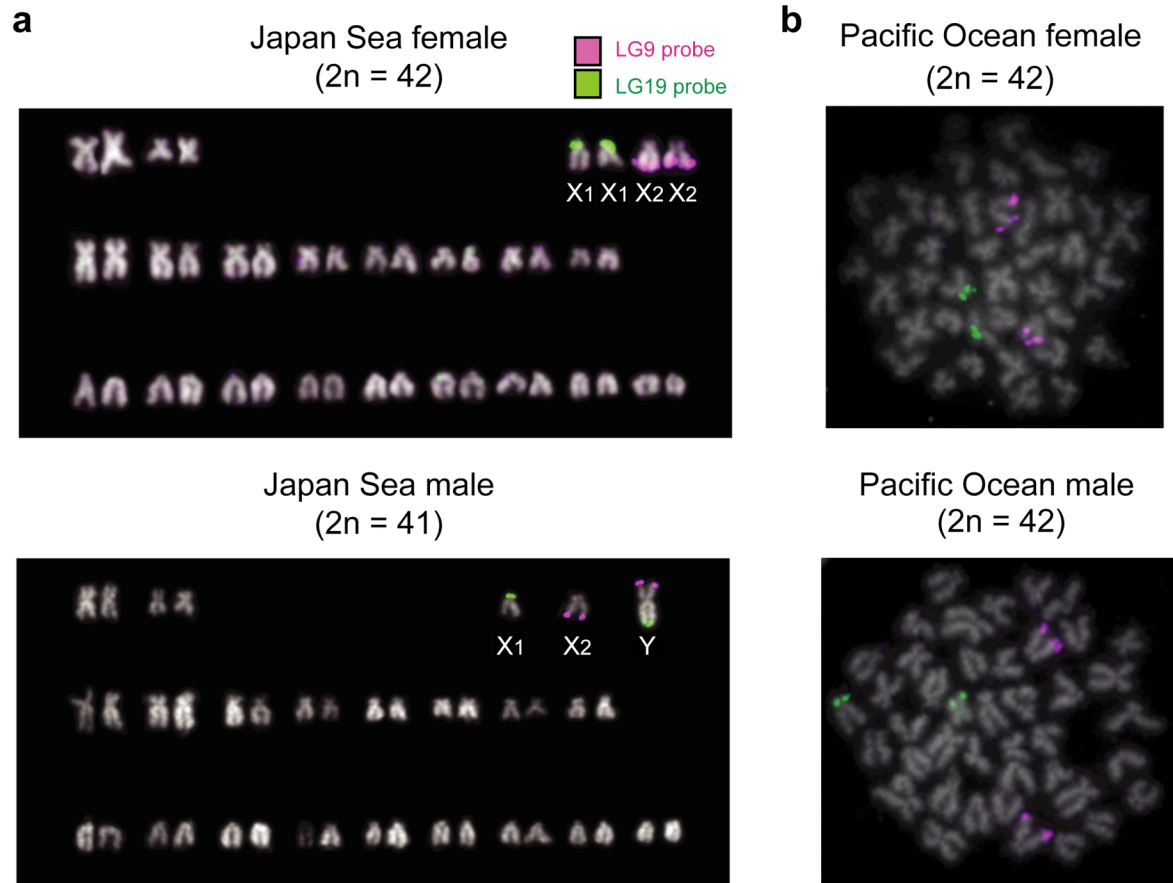
Although there is strong geographical isolation in the Bekanbeushi River system (Supplementary Fig. 3a), it is not complete, leading to a hybrid zone in the river (Fig. 2). In the hybrid zone, temporal isolation and behavioural isolation play important roles in reproductive isolation between Pacific Ocean females and Japan Sea males (Supplementary Fig. 3a). In contrast, hybrid male sterility plays an important role in reproductive isolation between Japan Sea females and Pacific Ocean males in the hybrid zone (Supplementary Fig. 3a).

In the hybrid zone, the sequential action of temporal and behavioural isolation is expected to completely prevent Pacific Ocean females from mating with Japan Sea males (Supplementary Fig. 3b). Therefore, no hybrids are expected to result from such crosses. In contrast, because of the absence of prezygotic barriers between Japan Sea females and Pacific Ocean males, as well as the presence of a large number of Pacific Ocean males in the hybrid zone, the majority (93.5%) of the progeny of Japan Sea females in the hybrid zone are expected to be F1 hybrids. In the hybrid zone, there are also more Pacific Ocean females (82/86) than Japan Sea females (4/86). Therefore, when the expected fraction of F1 hybrids from Japan Sea females (0.935) is multiplied by the relative frequency of the Japan Sea females (4/86), the expected frequency of F1 hybrid juveniles in the natural hybrid zone is only 0.0435. This expected value was close to the observed frequency of F1 hybrids (hybridity > 0.4): 0.0571 in 2006 and 0.0198 in 2007.

To further confirm the presence of prezygotic isolation within the hybrid zone, we compared the observed mean hybridity of juveniles in the hybrid zone with the expected mean hybridity estimated under random mating of the adult fish in the hybrid zone. The observed mean hybridity (0.0457 for 2006 and 0.0185 for 2007) was significantly lower than the expected mean hybridity (95% CI = 0.0527-0.143 for 2006 and 0.230-0.233 for 2007), suggesting that there is prezygotic isolation or early postzygotic isolation between these two forms in the hybrid zone.

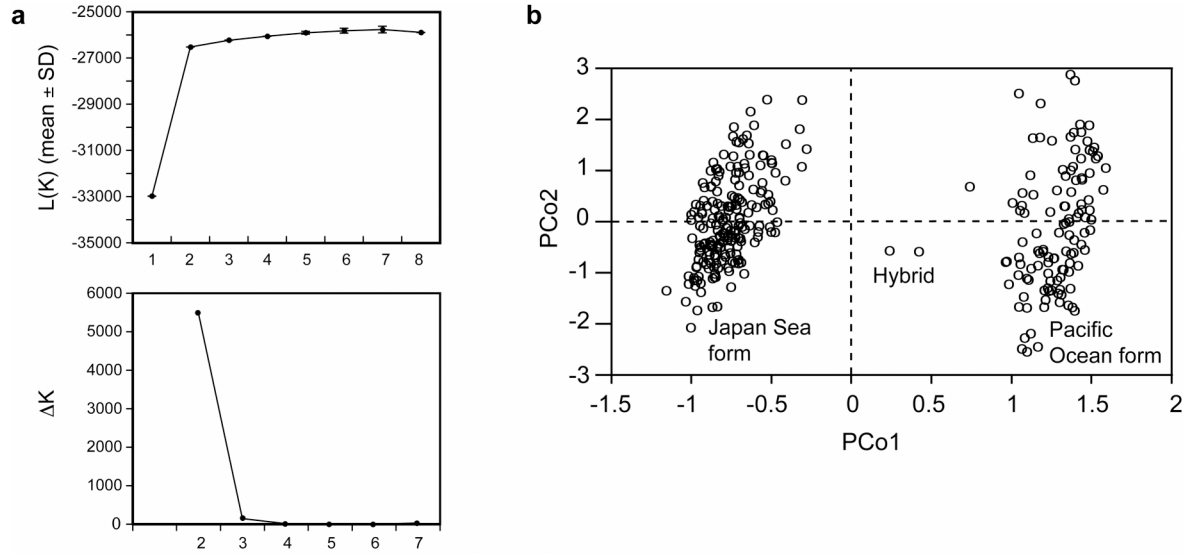
Hybrid inviability at early stages does not likely contribute to reproductive isolation in the hybrid zone because no significant reduction in hatching rate was found in either reciprocal hybrid cross<sup>49</sup>. To look for evidence of postzygotic isolation after the juvenile stage, we compared the frequencies of juvenile and adult hybrids. Although F1 (hybridity > 0.4) juveniles (6/457) were more common than F1 adults (1/422; Fig. 2), the difference was not statistically significant (two-tailed Fisher's exact test,  $P = 0.145$ ). When we included backcrossed hybrids (hybridity > 0.1), there were significantly more hybrid juveniles (17/547) than hybrid adults (2/422; two-tailed Fisher's exact test,  $P = 0.0037$ ). Thus, there might be postzygotic isolation at the post-juvenile stage. However, we cannot determine whether this results from selection against hybrids (extrinsic isolation) or genetic incompatibilities that only manifest at later stages of development (intrinsic isolation). Because lower hybrid fitness is thought to drive the evolution of prezygotic isolating barriers<sup>56</sup>, future studies will address the role of postzygotic hybrid inviability in reproductive isolation between the sympatric Japanese species pair.





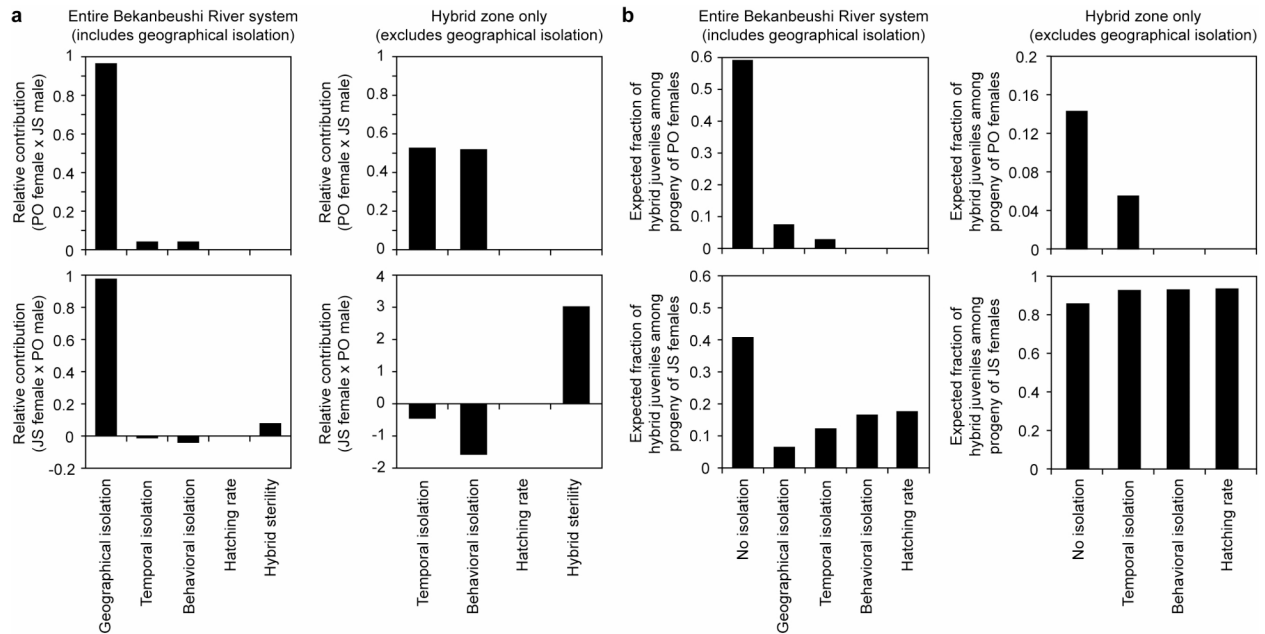
**Supplementary Figure 1 | Cytogenetic analysis of the Japan Sea and Pacific Ocean forms.**

**a**, Representative karyograms of a Japan Sea male and a Japan Sea female from Akkeshi, Japan. Metaphase chromosome spreads were hybridized with a LG9 probe (magenta) and a LG19 probe (green). Two Japan Sea males and one Japan Sea female were analyzed. We also confirmed these data in allopatric Japan Sea males ( $n = 2$ ) and females ( $n = 3$ ). **b**, Representative FISH images of a Pacific Ocean male and a Pacific Ocean female from Akkeshi, Japan, are shown. The LG19 probe (green) hybridizes to one submetacentric chromosome (X chromosome) and to one metacentric chromosome (Y chromosome) in males, as seen previously<sup>22</sup>. The LG9 probe (magenta) hybridizes to two submetacentric chromosomes in both males and females.

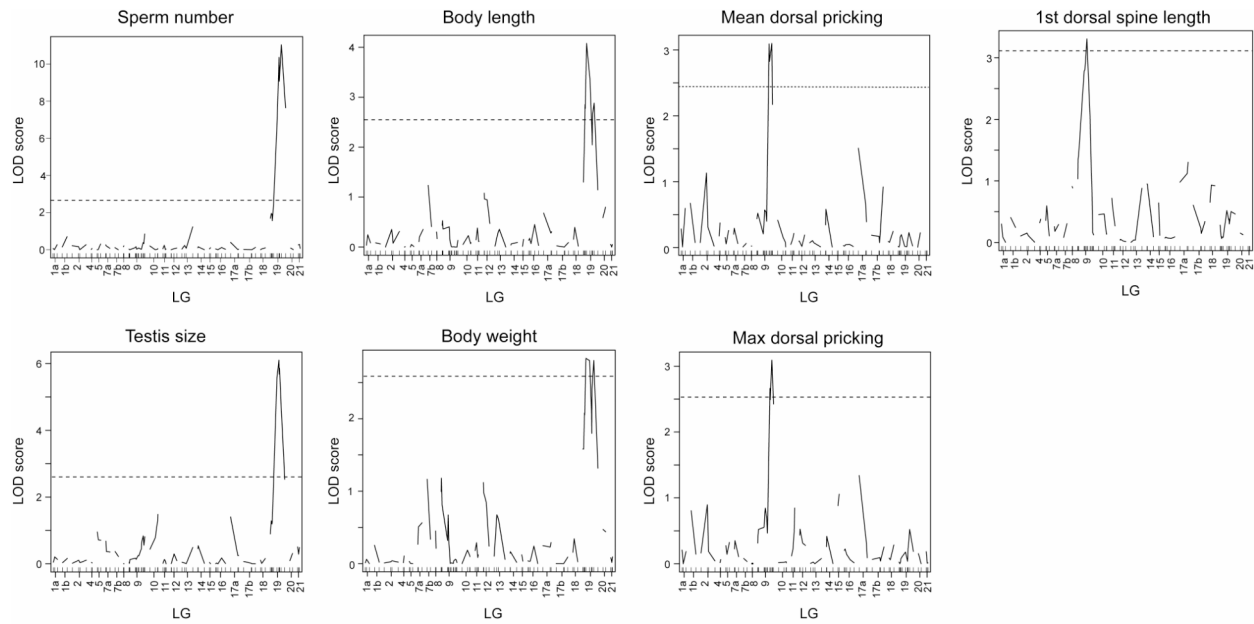


**Supplementary Figure 2 | Number of genetic clusters of threespine sticklebacks in Akkeshi.**

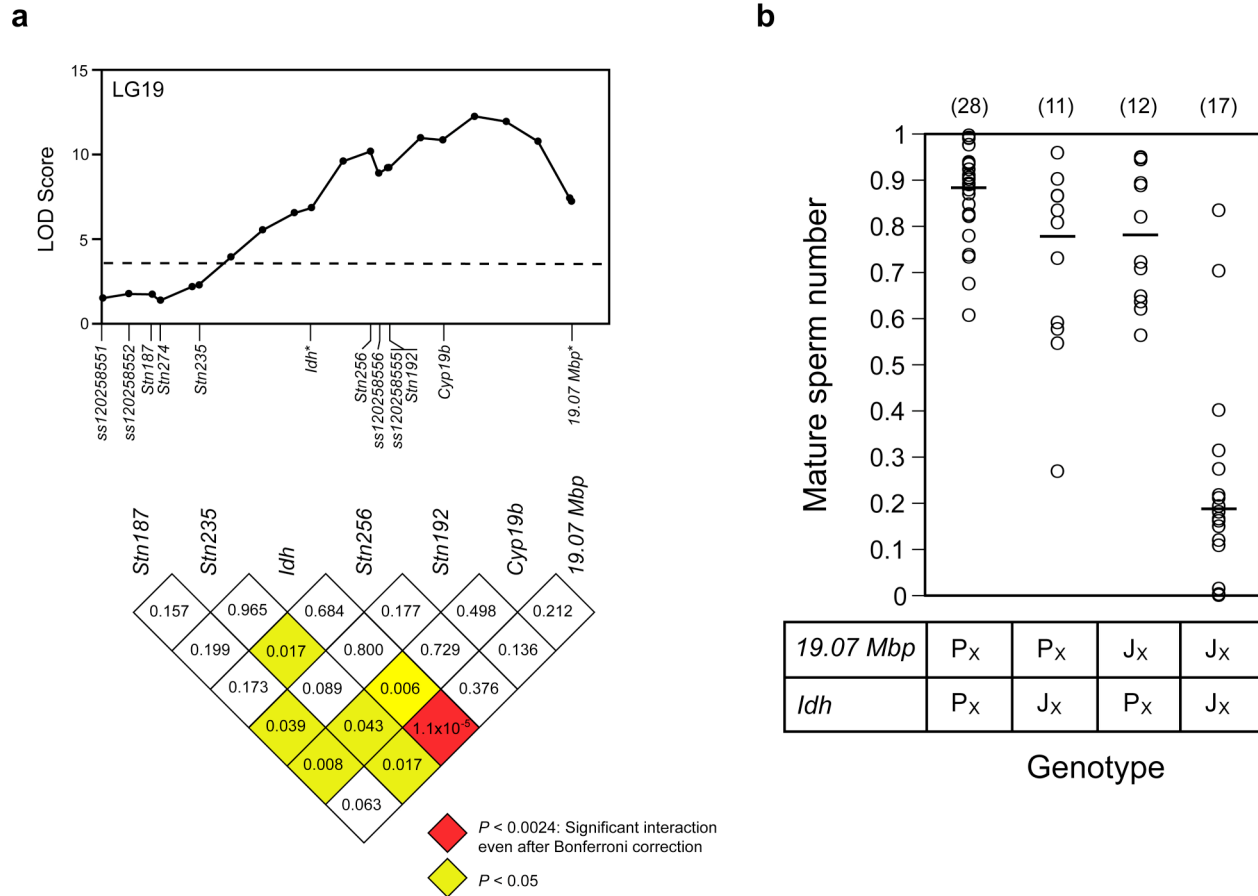
**a**, Estimation of genetic cluster number ( $K$ ) with STRUCTURE software was performed on fish (adults and juveniles) collected from all four sites in 2006 ( $n = 601$ ). Three simulations were conducted for  $K = 1$  through  $K = 8$ . The mean  $\pm$  SD of the log probability of data,  $L(K)$  is shown in the upper panel, and the *ad hoc* statistic  $\Delta K$  is shown in the lower panel. The plateau of  $L(K)$  and peak of  $\Delta K$  occur at  $K = 2$ , suggesting that two is the most probable number of genetic clusters in Akkeshi threespine sticklebacks. **b**, Two genetic clusters with a few potential hybrids were visualized by a scatterplot between the first (PCo1) and second (PCo2) principal coordinate scores of the genetic distance matrix of adults collected from all four sites in 2006 ( $n = 317$ ).



**Supplementary Figure 3 | Components of reproductive isolation and expected fraction of hybrids between sympatric threespine sticklebacks in Akkeshi.** **a**, The relative contribution of each isolating barrier to total isolation<sup>42</sup>. Relative contributions were calculated separately for isolation between Pacific Ocean (PO) females and Japan Sea (JS) males (upper panels) and Japan Sea (JS) females and Pacific Ocean (PO) males (lower panels). The left panels indicate the components of reproductive isolation including geographical isolation. The right panels indicate the components of reproductive isolation excluding geographical isolation, which corresponds to the isolating barriers present in the hybrid zone. **b**, Expected fraction of F1 hybrids after the sequential action of each isolating barrier<sup>50</sup>. The upper panel indicates the expected fraction of F1 hybrids among progeny of Pacific Ocean females, while the lower panel indicates the expected fraction of F1 hybrids among progeny of Japan Sea females. The left panels indicate the expected fraction of hybrids in the entire Bekanbeushi River system, while the right panels indicate the expected fraction of hybrids within the hybrid zone. These values are not adjusted to account for the relative frequency of Pacific Ocean and Japan Sea females within the hybrid zone.

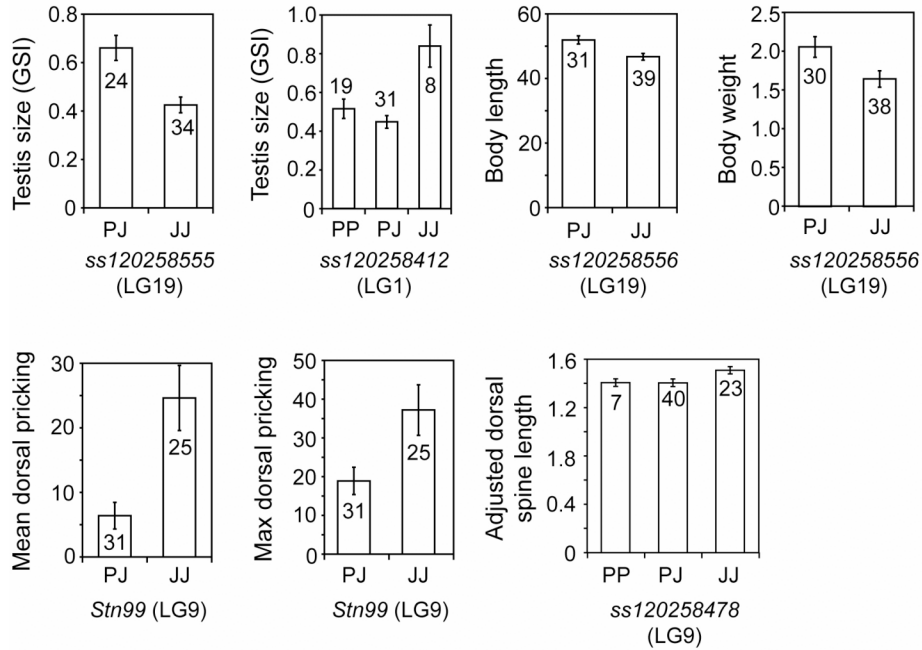


**Supplementary Figure 4 | QTL mapping using R/qtl in the backcross.** The LOD scores for sperm number, testis size, body length, body weight, mean dorsal pricking, max dorsal pricking, and first dorsal spine length are shown relative to the stickleback linkage groups (LG). LG3 and LG6 are not represented because linkage maps could not be made with the data for this cross. Due to the small cross size, markers from LG1, LG7 and LG17 each formed two linkage groups, which we designate as “a” and “b”. Genome-wide significance thresholds ( $\alpha = 0.05$ ) for each trait are indicated with a dashed horizontal line.

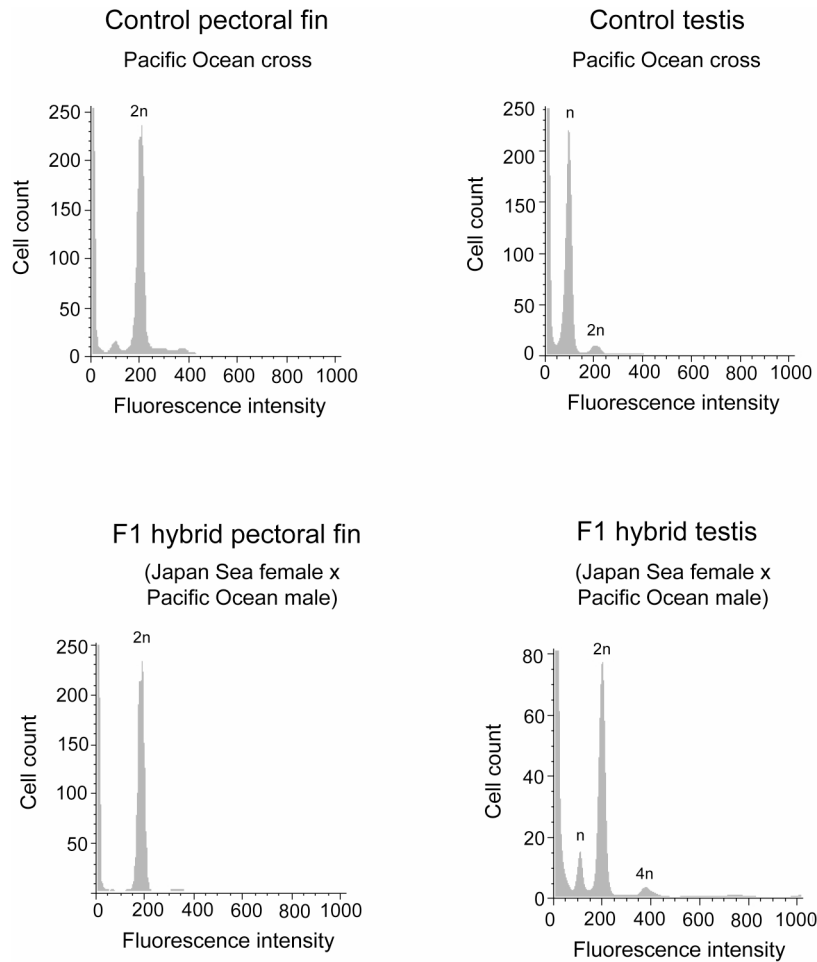


**Supplementary Figure 5 | Conspecific epistatic interactions between two genomic regions on the X underlie hybrid male sterility.** **a**, In the top panel, the LOD scores for the sperm number trait are plotted against the marker position in the LG19 backcross genetic map. The dashed line indicates the genome-wide significance threshold determined by permutation tests ( $\alpha = 0.05$ ). The  $P$ -values for each pairwise interaction were calculated by ANOVA and are shown below the LOD score map. The red square indicates a significant interaction even after Bonferroni correction, while the yellow squares indicate a suggestive interaction that is not significant after Bonferroni correction. Before ANOVA, sperm number was arcsine-transformed to meet the assumptions of normal distribution and homogeneity of variances. **b**, The number of mature sperm in each backcross male is indicated with a circle, and the males are clustered in columns according to genotype at two loci on LG19. Backcross males that have inherited Japan Sea alleles at two loci on the X chromosome (with a Pacific Ocean Y chromosome) show a significant reduction of mature sperm cells. Numbers of males in each genotypic class are indicated in parenthesis at the top of the graph. The horizontal bars indicate the mean phenotypes for each genotype. These data demonstrate that hybrid males suffer no sterility when they carry a Japan Sea allele at only one of the two loci, while hybrid males carrying Japan Sea alleles at both loci are sterile. This two-locus model with an interaction explains 70% of the phenotypic variance in mature sperm number in the backcross.





**Supplementary Figure 6 | QTL mapping in the F2 intercross.** Phenotype-genotype associations in F2 males. For each trait, the phenotypic values (mean  $\pm$  s.e.m.) are indicated for genotypes at the marker closest to the QTL peak. Sample sizes for each genotypic class are shown in the graph. The “sperm number” trait could not be mapped in this cross because we did not perform flow cytometry on the F2 male testes. Of the 70 F2 males genotyped, testis size and body weight data were not available for two males, and dorsal pricking data could not be obtained for 14 males. Note that F2 males cannot be homozygous for Pacific Ocean derived alleles at LG9 and LG19 markers that are derived from the non-recombining region of the Japan Sea Y chromosome that is segregating in this cross.



**Supplementary Figure 7 | Representative images of flow cytometry analysis of testis and pectoral fin.** The X-axis indicates the fluorescence intensity of DAPI, a DNA-binding dye, and the Y-axis indicates the number of cells. Pectoral fins from a control fish (Pacific Ocean cross) and a F1 hybrid fish (Japan Sea female x Pacific Ocean male) have a peak indicative of diploid cells (2n). A testis from a breeding Pacific Ocean male has a strong haploid (1n) peak, which corresponds to mature sperm. By contrast, the testis of a breeding hybrid male (Japan Sea female x Pacific Ocean male) has large peak at 2n, and a small peak at 1n, indicating that this hybrid has a reduced number of mature sperm. There are also a small number of tetraploid (4n) cells, indicating a possible block in meiosis.

**Supplementary Table 1 | Location and magnitude of effect for backcross QTL**

Trait	LG	Marker	Position		LOD	PVE	Mean ( $\pm$ s.e.m.)	
			cM	Mbp			PP	JP
Sperm number**	19	<i>Cyp19b</i>	53.6	16.67	11.03	52.6	0.88 (0.018)	0.43 (0.054)
Sperm number**	19	<i>Stn256</i>	42.2	13.66	10.36	50.6	0.86 (0.020)	0.42 (0.058)
Testis size**	19	<i>Stn256</i>	42.2	13.66	6.11	34.0	0.77 (0.041)	0.46 (0.036)
Body length**	19	<i>Stn235</i>	15.2	7.40	3.54	20.7	52.1 (0.82)	47.5 (0.72)
Body weight*	19	<i>Stn235</i>	15.2	7.40	2.83	16.8	1.88 (0.07)	1.49 (0.07)
Mean dorsal pricking**	9	<i>ss120258472</i>	72.8	4.88	3.02	23.1	2.12 (1.77)	12.6 (2.33)
Max dorsal pricking*	9	<i>Stn113</i>	69.2	5.18	3.09	23.1	8.87 (2.38)	25.9 (4.03)
First dorsal spine length†	9	<i>Stn108</i>	44.3	9.53	3.31	45.8	1.25 (0.003)	1.39 (0.025)

The genetic position of each marker closest to a QTL peak is given in cM and the physical position in the genome assembly ([http://www.ensembl.org/Gasterosteus\\_aculeatus/Info/Index](http://www.ensembl.org/Gasterosteus_aculeatus/Info/Index); Broad S1, Feb 2006) is given in Mbp. Because the order of the LG19 sequence assembly is inverted after 3.822 Mbp, physical locations on LG19 are based on Ross & Peichel<sup>22</sup>. The LOD scores and percent variance explained (PVE) is shown for the marker closest to the QTL peak. Differences in phenotype means between genotype classes were analyzed with the Kruskal-Wallis test.

\*\*  $P < 0.0001$  (significant after Bonferroni correction); \*  $P < 0.001$

† First dorsal spine length was always analyzed with body length as an interacting covariate after ln-transformation. There was a significant effect of *Stn108* genotype on dorsal spine length (ANCOVA,  $P = 0.014$ ) as well as a significant difference in the relationship between spine length and standard length between genotypes (ANCOVA,  $P = 0.017$ ). Mean ( $\pm$  s.e.m.) of ln-first dorsal spine length adjusted to the grand mean of ln-standard length is shown here.

Supplementary Table 2 | Location and magnitude of effect for F2 QTL

Trait	LG	Marker	Position		LOD	PVE	Mean ( $\pm$ s.e.m.)		
			cM	Mbp			PP	PJ	JJ
Testis size <sup>***</sup>	19	<i>ss120258555</i>	35.0	14.42	3.33 <sup>†</sup>	21.9	-	0.660 (0.052)	0.425 (0.032)
Testis size <sup>**</sup>	1	<i>ss120258412</i>	0	3.49	4.36 <sup>†</sup>	26.3	0.514 (0.049)	0.446 (0.032)	0.809 (0.102)
Body length <sup>**</sup>	19	<i>ss120258556</i>	32.9	13.0	2.19	12.1	-	51.9 (6.99)	46.7 (6.36)
Body weight <sup>*</sup>	19	<i>ss120258556</i>	32.9	13.0	1.28	6.9	-	2.06 (0.151)	1.65 (0.948)
Mean dorsal pricking <sup>**</sup>	9	<i>Stn99</i>	34.0	2.13	2.57 <sup>†</sup>	18.5	-	6.39 (2.06)	24.6 (5.04)
Max dorsal pricking	9	<i>Stn99</i>	34.0	2.13	1.52	10.1	-	17.5 (3.74)	34.6 (7.05)
First dorsal spine length <sup>‡</sup>	9	<i>ss120258478</i>	14.2	18.9	2.34	50.4	1.41 (0.031)	1.40 (0.031)	1.51 (0.031)

The genetic position of each marker closest to a QTL peak is given in cM and the physical position in the genome assembly ([http://www.ensembl.org/Gasterosteus\\_aculeatus/Info/Index](http://www.ensembl.org/Gasterosteus_aculeatus/Info/Index); Broad S1, Feb 2006) is given in Mbp. Because the order of the LG19 sequence assembly is inverted after 3.822 Mbp, physical locations on LG19 are based on Ross & Peichel<sup>22</sup>. The LOD scores and percent variance explained (PVE) is shown for the marker closest to the QTL peak. Differences in phenotype means between genotype classes were analyzed with the Kruskal-Wallis test.

\*\*\*  $P < 0.0005$ ; \*\*  $P < 0.005$ ; \*  $P < 0.05$ ; Max dorsal pricking was not significant ( $P = 0.070$ ).

<sup>†</sup>LOD score was higher than the threshold calculated by genome-wide permutation ( $\alpha = 0.05$ ).

For the non-recombining regions of the X-chromosome (LG9 and LG19), an X-chromosome-specific threshold was used<sup>55</sup>.

<sup>‡</sup>First dorsal spine length was always analyzed with body length as an interacting covariate after ln-transformation. The effect of SNP *ss120258478* genotype on dorsal spine length was close to significance (ANCOVA,  $P = 0.060$ ), and the difference in the relationship between spine length and standard length between genotypes was also close to significance (ANCOVA,  $P = 0.070$ ).

Mean ( $\pm$  s.e.m.) of ln-first dorsal spine length adjusted to the grand mean of ln-standard length is shown here.

**Supplementary Table 3 | No evidence for sex ratio meiotic drive**

Cross type	Number of dead eggs	Number of hatched eggs	Hatching rate (%)	Male:Female <sup>†</sup>	% Male
PP female x JP male	53	23	30.3	9:14	39.1
PP female x JP male	93	57	38.0	25:32	43.8
PP female x JP male	42	45	51.7	26:19	57.8
JS female x JP male	71	46	39.3	23:23	50.0
JP female x PP male <sup>*</sup>	NA	NA	NA	76:79	49.0
PJ female x PJ male <sup>*</sup>	NA	NA	NA	70:56	55.5

NA, not analyzed; PP, Pacific Ocean pure cross; JS, wild-caught Japan Sea fish; JP, F1 hybrid between Japan Sea female and Pacific Ocean male; PJ, F1 hybrid between Pacific Ocean female and Japan Sea male.

<sup>\*</sup>Sex ratios for the backcross (JP x PP) and the F2 intercross (PJ x PJ) used for QTL mapping are also shown in the table. Sex was determined in breeding adults by gonad inspection.

<sup>†</sup>Sex ratios were not biased in any cross ( $P > 0.05$ , two-tailed binomial test).



**Supplementary Table 4 | Microsatellite markers used for population genetic analysis**

Marker	LG	Range in bp* (number of alleles)	Most common allele (JS/PO) <sup>†</sup>	$H_o$ (JS/PO) <sup>‡</sup>	$H_e$ (JS/PO) <sup>‡</sup>
<i>Stn330</i>	1	156-204 (17)	186/182	0.82/0.40	0.87/0.38
<i>Stn384</i> <sup>§</sup>	1	96-134 (16)	106/130	0.56/0.82	0.52/0.78
<i>Stn8</i>	1	108-146 (21)	116/128	0.74/0.69	0.76/0.81
<i>Stn390</i>	3	192-200 (5)	196/194	0.53/0.01	0.53/0.01
<i>Stn46</i> <sup>§</sup>	4	230-286 (29)	250/234	0.89/0.68	0.94/0.64
<i>Stn238</i>	4	128-148 (11)	134/142	0.74/0.82	0.76/0.75
<i>Stn383</i> <sup>§</sup>	4	156-294 (16)	168/176	0.86/0.56	0.83/0.62
<i>Stn278</i> <sup>§</sup>	11	228-270 (19)	248/228	0.79/0.32	0.88/0.30
<i>Stn159</i>	13	166-250 (32)	188/186	0.91/0.84	0.95/0.87
<i>Stn233</i>	16	108-172 (31)	124/128	0.92/0.64	0.93/0.68
<i>Stn481</i>	18	152-226 (31)	160/204	0.74/0.91	0.81/0.95
<i>Stn389</i>	20	186-286 (49)	196/254	0.91/0.95	0.92/0.95

Data is based on a subset of adult fish collected in 2006, including 108 Japan Sea fish (probability of assignment to Japan Sea cluster by STRUCTURE > 0.95) collected in Lake Akkeshi and 77 Pacific Ocean fish (probability of assignment to Pacific Ocean cluster by STRUCTURE > 0.95) collected in the upstream region.

\*Range of allele sizes is shown in base pairs (bp).

<sup>†</sup>JS, Japan Sea form; PO, Pacific Ocean form.

<sup>‡</sup> $H_o$ , observed heterozygosity;  $H_e$ , expected heterozygosity.

<sup>§</sup>Species-diagnostic markers<sup>19</sup>.

**Supplementary Table 5 | SNP markers used for linkage mapping**

ssSNP	LG	Position	Cross
120258411	1	913033	Backcross, F2
120258412	1	3494580	Backcross, F2
120258413	1	7955458	Backcross
120258414	1	9345491	Backcross, F2
120258415	1	11963492	Backcross, F2
120258416	1	12038660	Backcross, F2
120258417	1	22361077	F2
120258418	2	533883	Backcross, F2
120258419	2	1388455	F2
120258420	2	3274866	F2
120258421	2	3384330	F2
120258422	2	3516452	F2
120258423	2	4530808	Backcross, F2
120258424	2	6300744	Backcross, F2
120258425	2	12292176	F2
120258426	2	16562987	Backcross, F2
120258427	2	20796189	Backcross
120258428	3	1198125	Backcross, F2
120258429	3	15856499	F2
120258430	3	16224572	F2
120258431	3	16251071	F2
120258432	4	4034002	F2
120258433	4	5313693	F2
120258434	4	10960835	F2
120258435	4	11367975	F2
120258436	4	12955826	F2
120258437	4	18425274	F2
120258438	4	23711481	F2
120258439	4	23804450	F2
120258440	4	23937349	F2
120258441	4	26191766	Backcross, F2
120258442	4	27614532	F2
120258443	4	29763654	F2
120258444	4	29846759	F2
120258445	4	32005807	F2
120258446	4	32378608	Backcross, F2
120258447	4	32387818	Backcross, F2
120258448	5	1238066	F2
120258449	5	2179756	Backcross, F2
120258450	5	9092208	Backcross, F2
120258451	5	9219138	Backcross, F2
120258452	5	11542501	Backcross, F2

120258453	5	11909552	Backcross, F2
120258454	6	11873663	F2
120258455	7	1521362	F2
120258456	7	2258224	Backcross, F2
120258457	7	5936068	Backcross, F2
120258458	7	17995892	Backcross
120258459	7	24203557	Backcross, F2
120258460	7	25662266	Backcross, F2
120258461	7	26227403	Backcross, F2
120258462	8	2923581	Backcross
120258463	8	3281178	F2
120258464	8	3987295	F2
120258465	8	4359755	Backcross, F2
120258466	8	17576018	F2
120258467	8	18432598	Backcross, F2
120258468	8	18685222	F2
120258469	8	19250570	F2
120258470	9	267823	Backcross
120258471	9	522899	Backcross, F2
120258472	9	4882924	Backcross
120258473	9	5189056	F2
120258474	9	5403530	Backcross
120258475	9	8719760	Backcross, F2
120258476	9	12255563	Backcross, F2
120258477	9	14076299	Backcross
120258478	9	18942598	F2
120258479	10	1245433	Backcross
120258480	10	1488158	F2
120258481	10	3419303	F2
120258482	10	4867730	Backcross
120258483	10	7113953	Backcross, F2
120258484	10	7790350	Backcross, F2
120258485	10	8703061	F2
120258486	10	14265366	Backcross, F2
120258487	11	234849	F2
120258488	11	1017481	Backcross
120258489	11	1449684	F2
120258490	11	1921360	Backcross, F2
120258491	11	3671630	Backcross, F2
120258492	11	5715882	Backcross, F2
120258493	11	14286902	Backcross
120258494	11	14616764	F2
120258495	11	16655205	F2
120258496	12	857247	Backcross, F2

120258497	12	1589655	F2
120258498	12	4322414	Backcross
120258499	12	5094466	Backcross
120258500	12	6913126	Backcross
120258501	12	8640908	Backcross, F2
120258502	13	879596	F2
120258503	13	1001571	Backcross, F2
120258504	13	1388673	Backcross, F2
120258505	13	2523163	Backcross
120258506	13	3109522	F2
120258507	13	3639405	Backcross
120258508	13	7266499	F2
120258509	13	9952376	Backcross, F2
120258510	13	17392141	F2
120258511	14	451065	F2
120258512	14	1442872	F2
120258513	14	1713227	F2
120258514	14	3414352	Backcross, F2
120258515	14	3534175	F2
120258516	14	3914017	Backcross, F2
120258517	14	11054767	F2
120258518	15	137728	Backcross
120258519	15	414608	Backcross, F2
120258520	15	8046107	F2
120258521	16	1677074	Backcross
120258522	16	2068005	Backcross, F2
120258523	16	2764206	F2
120258524	16	4537512	F2
120258525	16	10734565	Backcross, F2
120258526	16	12111717	Backcross, F2
120258527	16	13921749	Backcross
120258528	16	16673569	F2
120258529	16	18106789	Backcross
120258530	17	697462	Backcross, F2
120258531	17	950518	Backcross
120258532	17	2232080	F2
120258533	17	2416887	Backcross, F2
120258534	17	3843835	F2
120258535	17	11855617	Backcross
120258536	17	12022612	Backcross, F2
120258537	17	13481178	F2
120258538	17	14583681	Backcross, F2
120258539	18	4836241	Backcross, F2
120258540	18	5765162	F2

120258541	18	8193702	Backcross
120258542	18	11086837	F2
120258543	18	11765327	Backcross, F2
120258544	18	11843439	F2
120258545	18	12818939	F2
120258546	18	13352631	F2
120258547	18	13621127	F2
120258548	18	14415132	F2
120258549	18	15478444	F2
120258550	19	728155	F2
120258551	19	1472847	Backcross
120258552	19	1689208	Backcross
120258553	19	3309372	F2
120258554	19	8190806	F2
120258555	19	9639539	Backcross, F2
120258556	19	11034323	Backcross, F2
120258557	19	16088155	F2
120258558	19	18045399	F2
120258559	20	10841857	Backcross, F2
120258560	20	14324175	Backcross, F2
120258561	20	16328884	F2
120258562	21	3772258	Backcross
120258563	21	8268451	F2
120258564	21	10007883	Backcross, F2
120258565	21	10511282	Backcross, F2
120258566	21	11060209	Backcross
120258567	21	11414383	F2
120258568	27	2776586	Backcross, F2
120258569	54	12390868	F2
120258570	69	17922401	Backcross, F2
120258571	88	21213332	Backcross, F2
120258572	114	26026523	Backcross, F2
120258573	137	30545876	Backcross, F2
120258574	159	33627890	F2
120258575	178	36625247	F2
120258576	195	38378170	F2

For each SNP used for linkage mapping in the backcross and/or the F2 intercross, the unique submitted SNP (ssSNP) number is provided so that complete SNP information can be accessed at NCBI dbSNP (<http://www.ncbi.nlm.nih.gov/projects/SNP/>). The chromosomal location (LG) and position in base pairs on the LG of the SNP is also provided and is based on the *G. aculeatus* genome assembly (Broad S1, Feb 2006). All LG numbers higher than 21 refer to sequence scaffolds that have not yet been incorporated into the linkage group assemblies.



## SUPPLEMENTARY NOTES

36. Kume, M., Kitamura, T., Takahashi, H. & Goto, A. Distinct spawning migration patterns in sympatric Japan Sea and Pacific Ocean forms of threespine stickleback, *Gasterosteus aculeatus*. *Ichthyol. Res.* **52**, 189-193 (2005).
37. Raymond, M. & Rousset, F. GENEPOP, version 1.2: population genetics software for exact tests and ecumenicism. *J. Hered.* **86**, 248-249 (1995).
38. Pritchard, J. K., Stephens, M. & Donnelly, P. Inference of population structure using multilocus genotype data. *Genetics* **155**, 945-959 (2000).
39. Evanno, G., Regnaut, S. & Goudet, J. Detecting the number of clusters of individuals using the software STRUCTURE: a simulation study. *Mol. Ecol.* **14**, 2611-2620 (2005).
40. Dieringer, D. & Schlötter, C. Microsatellite analyzer (MSA): a platform independent analysis tool for large microsatellite data sets. *Mol. Ecol. Notes* **3**, 167-169 (2003).
41. R Development Core Team. R: a language and environment for statistical computing. R Foundation for Statistical Computing, Vienna, Austria (2006).
42. Ramsey, J., Bradshaw, H. D. & Schemske, D. W. Components of reproductive isolation between the monkeyflowers *Mimulus lewisii* and *M. cardinalis* (Phrymaceae). *Evolution* **57**, 1520-1534 (2003).
43. Coyne, J. A. & Orr, H. A. Patterns of speciation in *Drosophila*. *Evolution* **43**, 362-381 (1989).
44. Nosil, P., Vines, T. H. & Funk, D. J. Reproductive isolation caused by natural selection against immigrants from divergent habitats. *Evolution* **59**, 705-719 (2005).
45. Whiteman, H. H. & Semlitsch, R. D. Asymmetric reproductive isolation among polymorphic salamanders. *Biol. J. Linn. Soc.* **86**, 265-281 (2005).
46. Kay, K. M. Reproductive isolation between two closely related hummingbird-pollinated neotropical gingers. *Evolution* **60**, 538-552 (2006).
47. Kume, M. Divergence of life history and reproductive isolation between Japan Sea and Pacific Ocean forms of threespine stickleback. *Ph.D. thesis* (Hokkaido Univ., Hokkaido, 2007).
48. Yamada, M. Evolutionary process and introgression of mitochondrial DNA in threespine stickleback, *Gasterosteus aculeatus*, around Japan. *Ph.D. thesis* (Hokkaido Univ., Hokkaido, 2003).
49. Yamada, M. & Goto, A. *Natural History of Stickleback* (eds Goto, A. & Mori, S.) 90-101 (Hokkaido Univ. Press, Hokkaido, 2003).
50. Martin, N. H. & Willis, J. H. Ecological divergence associated with mating system causes nearly complete reproductive isolation between sympatric *Mimulus* species. *Evolution* **61**, 68-82 (2007).
51. McKinnon, J. S. *et al.* Evidence for ecology's role in speciation. *Nature* **429**, 294-298 (2004).
52. Schluter, D. Estimating the form of natural selection on a quantitative trait. *Evolution* **42**, 849-861 (1988).
53. Akaike, H. A new look at the statistical model identification. *IEEE Trans. on Automat. Contr.* **19**, 716-723 (1974).
54. Murphy, B. R. & Willis, D. W. *Fisheries Techniques* (American Fisheries Society, Bethesda, 1996).
55. Broman, K. W. *et al.* The X chromosome in quantitative trait locus mapping. *Genetics* **174**, 2151-2158 (2006).
56. Dobzhansky, T. *Genetics and the Origin of Species* (Columbia Univ. Press, New York, 1951).